

The Potts Fully Frustrated model: Phase diagram and dynamical behavior

Giancarlo Franzese *

Dip. di Scienze Fisiche, Università di Napoli, Mostra d'Oltremare Pad.19 I-80125 Napoli, Italy

Dip. di Fisica "E. Amaldi", Università Roma Tre, via della Vasca Navale 84, I-00146 Roma, Italy

Istituto Nazionale per la Fisica della Materia - unità di Napoli Mostra d'Oltremare Pad.19 I-80125 Napoli, Italy

(February 21, 2019)

Recent numerical results have shown that dynamical anomalies typical of glasses, like non-exponential correlation functions, occur in the paramagnetic phase of frustrated systems without disorder. The introduction of a generalization of a fully frustrated (FF) Ising model, the Potts FF model, shows that they can be related to a Potts transition. The model describes frustrated systems with orientational degrees of freedom like, for example, structural glasses. In this paper the model is studied in detail with a cluster Monte Carlo dynamics, showing that the Potts transition coincides with a percolation transition. The dynamics of the model near this Potts/percolation transition is studied by means of spin-flip dynamics, showing that this transition numerically coincides with the onset of non-exponential autocorrelation functions. This could be relevant in the interpretation of recent experimental results on complex liquids and structural glasses.

PACS numbers: 05.70.Fh, 64.60.Ak, 67.57.Lm, 02.70.Lq

I. INTRODUCTION

Glassy systems [1] can be defined as materials characterized by a slowing down of one or more degrees of freedom [2,3] which prevents the system to reach the equilibrium as the temperature decreases. Although many steps toward their complete physical understanding have been done, many open questions are still present. The most common example of this category of systems are the real glasses that can be considered *strongly correlated* liquids in the sense that at low temperature they have a diverging viscosity. This strong correlation induces the slowing down of the motion of the liquid components, i.e. the divergence of the relaxation time τ of large-scale flow processes, and a complex dynamics characterized by non-equilibrium phenomena like *aging* [2,4]. Analogous complex behavior is seen in many other materials, like supercooled liquids, polymers, microemulsions, granular material, vortex glasses, ionic conductors, colloids, plastic glassy crystals and spin glasses (SGs) [1]. From the theoretical point of view an increasing attention has been devoted in the context of glassy dynamics to the study of SGs [5], which share many phenomenological aspects with *fragile* glasses [6], i.e. glasses whose τ diverges at finite temperature with marked deviation from Arrhenius behavior [2]. The nature of this analogies is still matter of debate [7,8].

SGs are dilute alloys of magnetic atoms in low concentration in a non-magnetic matrix. The relevant degrees of freedom in this case are the spins of the impurities interacting via random magnetic couplings due to the quenched disordered distribution of the impurities in the

matrix. The randomness gives rise to *frustration*, that is a competition that prevents the systems to minimize the global free energy to reach the equilibrium. SG models used in the context of glasses are for example the Potts glass [9], the p -spin SG [10] or the Potts spin glass [11–13]. In these models frustration and disorder are essential features of the systems [14].

Furthermore, the study of frustrated systems without quenched disorder [16], like fully frustrated (FF) Ising models [17], has shown that the presence of the sole frustration is enough to induce the glassy behavior [18,19]. The absences of disorder makes these models easier to study than the SGs and allows to clarify the role of frustration respect to disorder. Moreover, they are assuming an increasing experimental relevance related to the Josephson junction arrays [20].

One of the features shared by different glassy systems is the presence, well above the glass transition, of precursor phenomena, such as a dynamical transition from high temperatures exponential to low temperatures non-exponential autocorrelation functions [21]. This phenomenology is seen both in experiments on glasses [2] and on SGs [22].

From the theoretical point of view it is possible to see that in SGs precursor phenomena occur where the free energy of the systems has no singularity and that they are related to the Griffiths transition [23], that vanishes for vanishing external field [24]. It takes place as consequence of the presence of rare large unfrustrated spins regions, due to the randomness, that order themselves at the transition temperature of a pure ferromagnet. Numerical results confirm the theoretical prediction when

*Present address: Center for Polymer Studies, Boston University, Boston, Massachusetts 02215

disorder is present, both on a $\pm J$ Ising SG in 3 dimension (3D) [25] and on its generalization [13] with both Ising spins and s -states Potts variables [26], the s -states Potts SG (PSG) model [11,12].

On the other hand in the FF Ising model, due to the lack of disorder, the Griffiths transition is not defined, but the dynamical transition is still present [18]. Moreover the same dynamical transition is also seen in the generalization of the FF Ising model, i.e. the s -states Potts FF (PFF) model citebreve,FFdCC. As pointed out in Ref. [13], this dynamical transition in the PFF model can be related to a static transition.

In this paper we will study in details the statics of the PFF model and we will improve the results on its dynamics giving other evidences of the relation between dynamical anomalies and thermodynamics transition. In particular, we will show by means of cluster Monte Carlo (MC) dynamics, that the static transition, occurring above the standard FF transition, is in the universality class of a s -states ferromagnetic Potts transition that disappears only for the $s = 1$ case (FF Ising model) and that for any s coincides with a percolation transition [27]. Furthermore, to check the presence of the dynamical transition, we use a standard spin-flip dynamics and the calculations on the correlation function of the Potts order parameter confirm the presence of stretched exponential behavior. The main findings of this work are summarized by Figs. 15 and 18.

The model mimic the complex dynamic behavior of fragile glasses, like o-therphenyl [28] and should be relevant to explain some experimental results related to dielectric measurements in glass-forming liquids, like glycerol [29,30], or in structural glasses, like plastic glassy crystals [31]. Furthermore, it should be also of some interest in the interpretation of experimental data for microemulsions and porous glasses where the onset of non-exponential autocorrelation functions coincides with a percolation temperature [32].

In Sec. II we introduce the PFF model and the related cluster definition. In Sec. III we present the numerical phase diagram in 2D as result of the cluster MC dynamics simulation; the reader not interested in technical details can skip subsections III A and III B. In Sec. IV we use the spin-flip MC dynamics to study the dynamical transition. In Sec. V we give the summary and conclusions.

II. HAMILTONIAN AND CLUSTERS

The PFF model is introduced as a generalization of the FF Ising model [17] and is defined by the Hamiltonian

$$H\{S_i, \sigma_i\} = -sJ \sum_{\langle i,j \rangle} [\delta_{\sigma_i \sigma_j}(\epsilon_{i,j} S_i S_j + 1) - 2] \quad (1)$$

where the sum is extended over all the nearest-neighbor (NN) sites, $S_i = \pm 1$ is an Ising spin, $\sigma_i = 1, \dots, s$ is a

s -state Potts variable, J is the strength of interaction, $\epsilon_{i,j} = \pm 1$ is a quenched variable that represents the sign of the ferromagnetic/antiferromagnetic interaction and is distributed in a deterministic way such that each lattice cell is frustrated, i.e. has an odd number of -1 signs. In particular, we have considered a square lattice with alternate rows of ferromagnetic and antiferromagnetic interactions and with columns of ferromagnetic interactions as shown in Fig.1. The energy associated to each edge (or couple of NN sites) of the lattice depends on the state of both the Ising spins and the Potts variables on the sites connected by the edge. For example couples a, c, e and g in Fig.1 contribute with 0 energy, while couples b, d and f with $2sJ$ energy.

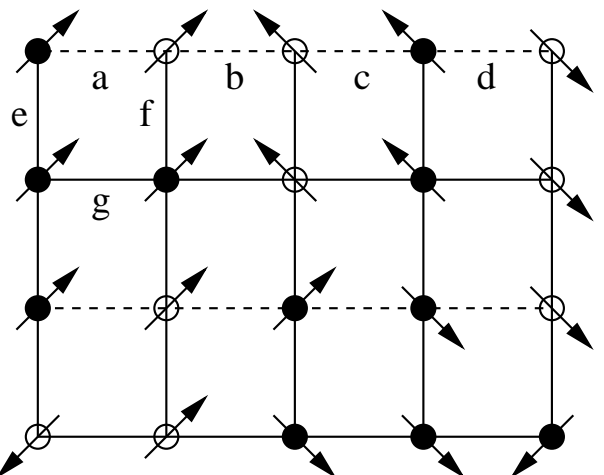


FIG. 1. Example of PFF model on a square lattice: on each vertex there is an Ising spin (represented by an open or a full dot depending on the state $+1$ or -1) and a Potts variable (in this example with $s = 4$ states represented by arrows pointing in 4 different directions). Potts variables interact via ferromagnetic couplings (not represented in the figure), while Ising spins interact via ferromagnetic or antiferromagnetic couplings (represented by full lines or dotted lines, respectively).

The model is a superposition of a ferromagnetic s -state Potts model [26] and a FF Ising model [17] and for $s = 1$ (i.e. $\delta_{\sigma_i \sigma_j} = 1$) recovers the FF Ising Hamiltonian. It can be considered as a model for structural glasses where on each lattice site there is a components (e.g. a molecule) with an orientational degree of freedom (the Potts variable) and which is frustrated (by means of frustrated Ising spins) for taking into account the effect due, for example, to steric hindrance. Examples of experimental systems with this feature are o-therphenyl or plastic glassy crystals.

The model has been studied within the mean field (MF) approximation in Ref. [33] giving a phase diagram qualitatively analogous to that obtained for the the PSG model by means of an analytical [34] and a numerical [12] approach. In this paper we study the numerical 2D

phase diagram of the PFF model, complementary to the MF results.

Analogously to the PSG case, it is possible to apply to the PFF model the Fortuin-Kasteleyn-Coniglio-Klein (FK-CK) [35] clusters formalism, rewriting the partition function Z in terms of bond configurations C [11]

$$Z \equiv \sum_{\{S_i, \sigma_i\}} e^{-H\{S_i, \sigma_i\}/k_B T} = \sum_C W_s(C) \quad (2)$$

where k_B is the Boltzmann constant, $W_s(C) = 0$ if C includes any frustrated loop (defined below), otherwise

$$W_s(C) = p^{|C|}(1-p)^{|A|}(2s)^{N(C)} \quad (3)$$

where $p = 1 - \exp[-2sJ/k_B T]$ is the probability to put a bond between two NN sites with both Ising spins and Potts variables minimizing the reciprocal interaction energy (e.g. the couples a, c, e and g in Fig. 1), $N(C)$ is the number of clusters (defined as maximal sets of connected bonds) in the configuration C , $|C|$ is the number of bonds and $|C| + |A|$ is total number of interactions. A loop of bonds is called frustrated if there is no Ising spin configuration able to satisfy all the interactions in the loop, i.e. if the product of all the signs of the interactions of the loop is equal to -1 (e.g. the loop a, e, g, f in Fig. 1). Notice that while the Hamiltonian in Eq. (1) is defined only for integer values of s , the Eq. (2) is meaningful for any value of s and can be interpreted as the partition function of a percolation model [18].

In 2D the case $s = 1$ (the FF Ising model) has an exact solution [17,36] with a second-order phase transition at $T_{FF} = 0$ and the FK-CK percolation temperature is $k_B T_p(s = 1)/J \simeq 1.69$ [37] consistent with the onset of dynamical anomalies [18]. Analogous results are available for the 3D $s = 1$ case [18]. In the following we will consider the case in 2D with $s > 1$.

III. NUMERICAL RESULTS IN 2D

To study the phase diagram of the s -state PFF model we have simulated the model for $s = 2, 7, 20, 50$ on square FF lattices with periodic boundary conditions (p.b.c.). Near $T_{FF} = 0$ the model behaves for any s like a standard FF Ising model with a FF transition at T_{FF} [17], since all the Potts spins tend to order. We are interested in understanding the phase diagram near the percolation transition occurring at $T_p(s) > T_{FF}$ [11]. In this temperature's region the Swendsen and Wang (SW) MC cluster dynamics [38], discussed in Ref. [12] and based on the FK-CK clusters defined in the previous section, is faster than standard local dynamics (like spin-flip dynamics). Therefore we have simulated the model with the SW dynamics using an annealing method, i.e. with a slow cooling of the system and taking the equilibrium

spin-configuration reached at each temperature as starting configuration for the successive temperature. The efficiency of the SW dynamics allows to average the data at each temperature over only 10^4 MC steps, defined as the update of the whole system, discarding the first 5×10^3 MC steps.

To distinguish between first-order and second-order phase transitions we have calculated for each s the Binder's parameter [39] for the energy density E defined as

$$V = 1 - \frac{\langle E^4 \rangle}{3\langle E^2 \rangle^2}, \quad (4)$$

where the angular brackets denote the thermal average. For a second-order phase transition in the limit $L \rightarrow \infty$ is $V = 2/3$ for all temperatures, while for a first-order phase transition V near the transition temperature has a well pronounced minimum related to the latent heat. To study the thermodynamic of the model we have calculated the Potts order parameter

$$M = \frac{s \max_i(M_i) - 1}{s - 1} \quad (5)$$

(where $i = 1, \dots, s$, M_i is the density of Potts spins in the i -th state), the fluctuations of M and E , i.e. the susceptibility

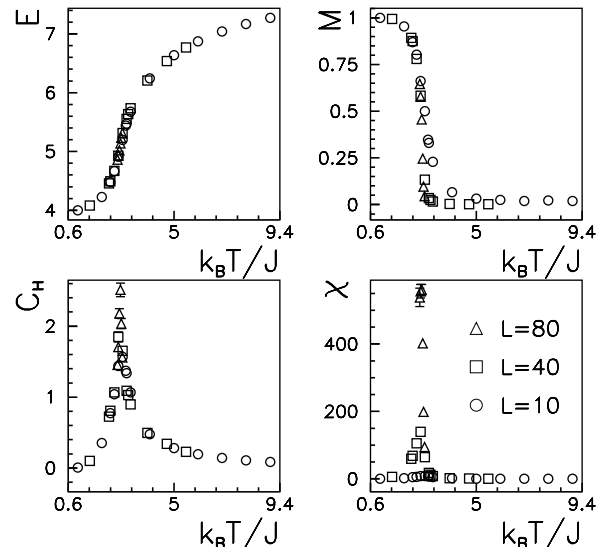


FIG. 2. PFF model with $s = 2$: Density of energy E , Potts order parameter M , specific heat C_H and susceptibility χ vs. temperature T . For clarity we show only data for lattice sizes $L = 10, 40, 80$. Where not shown, errors are smaller than symbols size.

$$\chi = \frac{1}{k_B T} \frac{\langle M^2 \rangle - \langle M \rangle^2}{N} \quad (6)$$

(where N is the total number of Potts spins) and the specific heat

$$C_H = \frac{1}{k_B T^2} \frac{\langle E^2 \rangle - \langle E \rangle^2}{N}. \quad (7)$$

To study the FK-CK percolation we have calculated the percolation probability per spin $P = 1 - m_1$, the mean cluster size $S = m_2$, the number of clusters $N_c = m_0$ (where

$$m_n = \sum_k k^n n_k \quad (8)$$

is the n -th moment of the distribution of density n_k of clusters with size k), the number of bonds per lattice site N_b , the mean size per lattice site of the largest (percolating) cluster S_I and of the second largest cluster S_{II} .

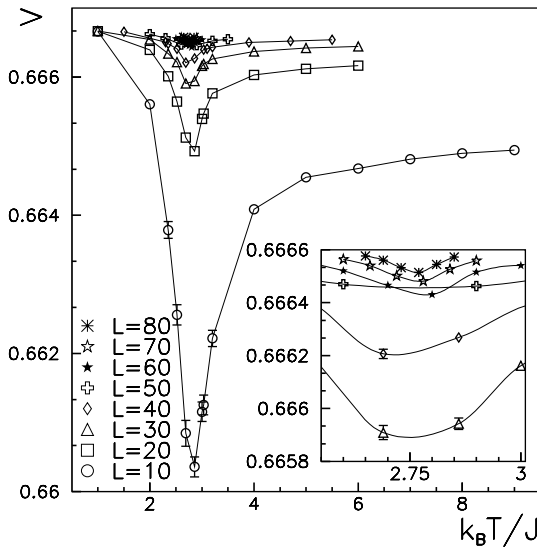


FIG. 3. PFF model with $s = 2$: Binder's parameter V vs. T for the lattice sizes L listed in the figure. Inset: Enlarged view. Where not shown, errors are smaller than symbols size. Lines are only guides for the eyes.

A. The second-order transition for $s = 2$

For the 2-states PFF model we have considered FF square systems with linear size L from 10 to 80 lattice steps. The calculated density of energy E , Potts order parameter M , specific heat C_H and susceptibility χ for some of these sizes are shown in Fig. 2. The Binder's parameter V goes to the constant value $2/3$ for all the temperatures as L increases, as shown in Fig. 3, revealing

a second-order phase transition. The transition temperature T_s in the thermodynamic limit can be estimated, together with all the critical exponents, using the standard scaling analysis [40] for second-order phase transition, where by definition of critical exponents ν , β , γ and α is

$$\xi \sim |T - T_s|^{-\nu}, \quad (9)$$

being ξ the correlation length,

$$M \sim |T - T_s|^\beta \sim \xi^{-\beta/\nu}, \quad (10)$$

$$\chi \sim |T - T_s|^{-\gamma} \sim \xi^{\gamma/\nu}, \quad (11)$$

$$C_H \sim |T - T_s|^{-\alpha} \sim \xi^{\alpha/\nu}, \quad (12)$$

for which we expect

$$M \sim L^{-\beta/\nu} f_M((T - T_s)L^{1/\nu}), \quad (13)$$

$$\chi \sim L^{-\gamma/\nu} f_\chi((T - T_s)L^{1/\nu}), \quad (14)$$

$$C_H \sim L^{\alpha/\nu} f_{C_H}((T - T_s)L^{1/\nu}), \quad (15)$$

where $f_M(x)$, $f_\chi(x)$ and $f_{C_H}(x)$ are universal functions of the dimensionless variable x . The values at which the hypothesis in Eqs. (13)-(15) are verified give the estimates of critical exponents and of T_s .

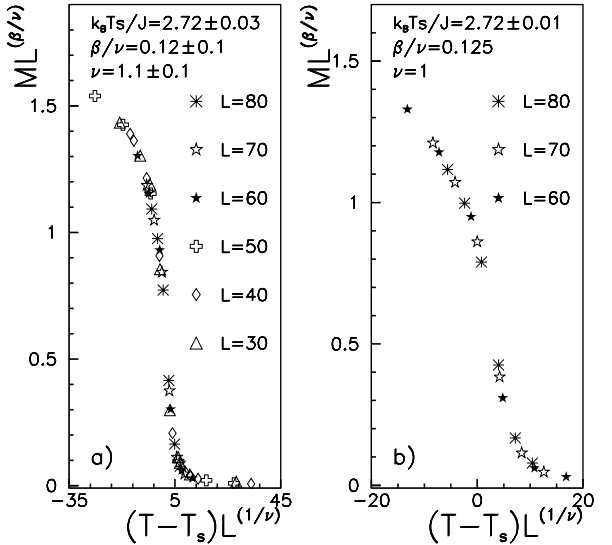


FIG. 4. PFF model with $s = 2$. Collapse of M data in Fig. 2: in panel a) for $L \geq 30$ with estimates of scaling parameters given in the figure; in b) for $L \geq 60$ for the Ising critical exponents and $k_B T_s/J = 2.72 \pm 0.01$ [41].

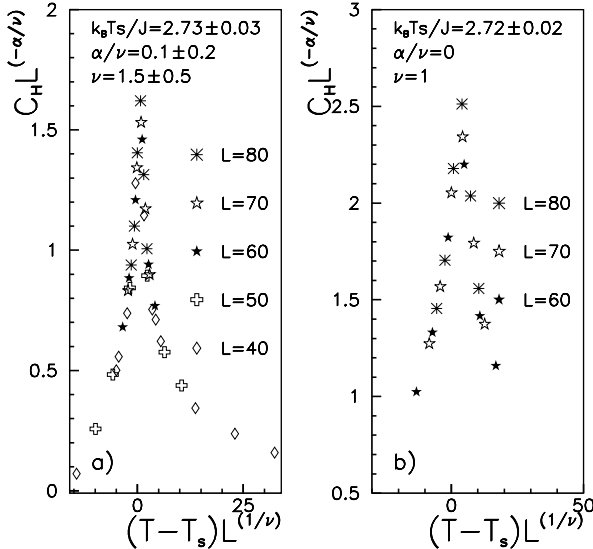


FIG. 5. PFF model with $s = 2$. Collapse of C_H data in Fig. 2: in panel a) for $L \geq 40$ with estimates of scaling parameters given in the figure; in b) for $L \geq 60$ for the Ising critical exponents and $k_B T_s/J = 2.72 \pm 0.02$ [41].

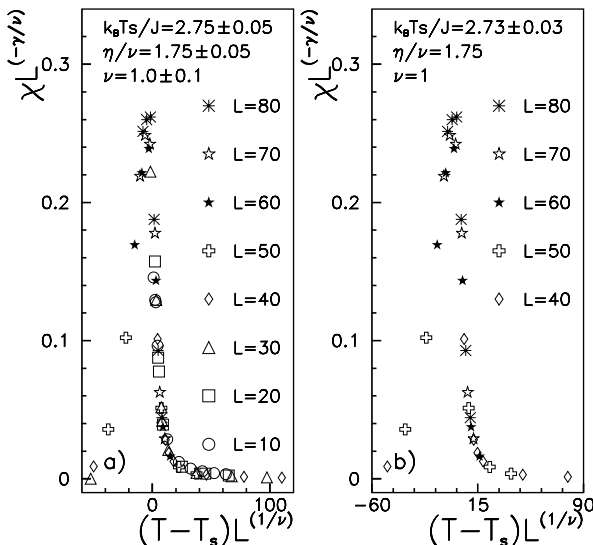


FIG. 6. PFF model with $s = 2$. Collapse of χ data in Fig. 2: in panel a) for $L \geq 10$ with estimates of scaling parameters given in the figure; in b) for $L \geq 40$ for the Ising critical exponents and $k_B T_s/J = 2.73 \pm 0.03$ [41].

In Figs. 4.a - 6.a we present the data collapses of all the data recorded (some of which are shown in Fig. 2), giving estimates of the scaling parameters and of the errors on them due to the finite size-effects. For comparison in Figs. 4.b - 6.b we present the collapses of the large-sizes data using the set of Ising critical exponents

[42] and leaving only T_s as free parameter. In this way we show the size above which the size-effects are negligible for the considered quantity. The estimated exponents are consistent, within the errors, to the critical exponents of the Ising model in 2D showing that the results of the MF approach [33] are qualitatively valid also at low dimension. Considering the large-size data collapses, it is possible to estimate the critical temperature as $k_B T_s/J = 2.73 \pm 0.03$.

The calculated percolation quantities are given in Fig. 7. Notice that at low temperatures there is only a percolating cluster with mean size equal to L^2 (see N_c , S_I and S_{II} in Fig. 7) and the density of bonds is less than one per site as consequence of the impossibility to close frustrated loops of bonds (see Sec.II).

From the smooth behavior of the percolation order parameter P one can make the ansatz that the percolation transition is of second-order and define a FK-CK percolation temperature T_p and a set of percolation critical exponents ν_p , β_p and γ_p by means of the relations

$$\xi_p \sim |T - T_p|^{-\nu_p} \quad (16)$$

where ξ_p is the connectedness length of the clusters (i.e. the typical linear cluster size) and

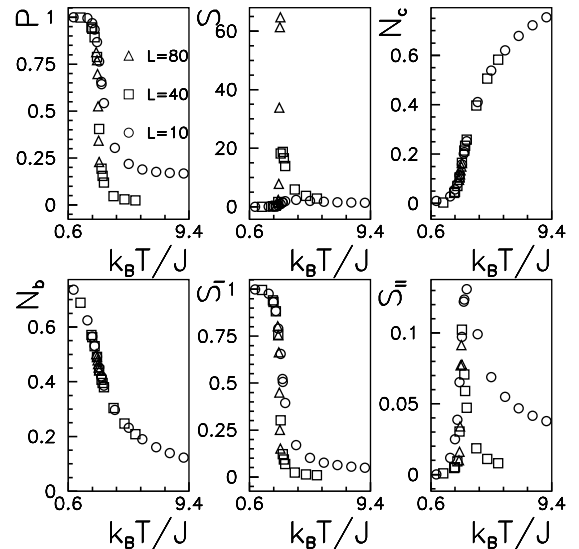


FIG. 7. PFF model with $s = 2$: Percolation probability per spin P , mean cluster size S , density of cluster N_c , density of bonds N_b , mean size per lattice site of largest cluster S_I and of second largest clusters S_{II} vs. temperature T . For clarity we show only data for lattice sizes $L = 10, 40, 80$. Errors are smaller than symbols size.

$$P \sim |T - T_p|^{\beta_p} \sim \xi_p^{-\beta_p/\nu_p}, \quad (17)$$

$$S \sim |T - T_p|^{-\gamma_p} \sim \xi_p^{\gamma_p/\nu_p}. \quad (18)$$

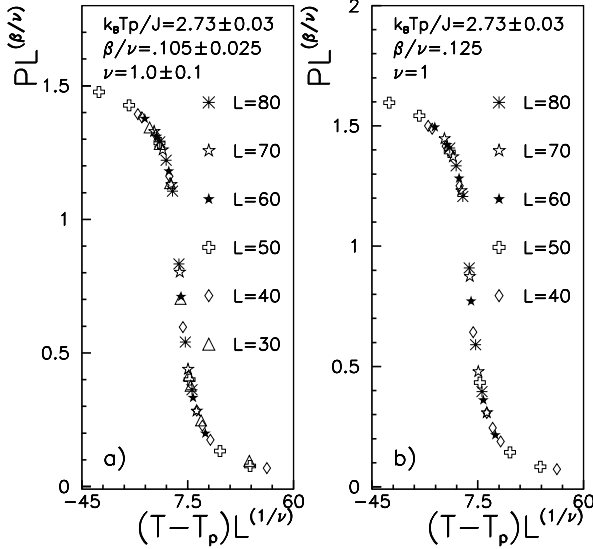


FIG. 8. PFF model with $s = 2$. Collapse of P data in Fig. 7: in panel a) for $L \geq 30$ with estimates of scaling parameters given in the figure; in b) for $L \geq 40$ for the Ising critical exponents and $k_B T_s/J = 2.73 \pm 0.03$ [41].

Applying the standard scaling analysis for percolation [43], one obtains in a consistent way the results summarized in Figs. 8, 9. All the estimated exponents are compatible, within the errors, to the corresponding thermodynamic parameters for the 2D Ising model and the numerical estimate for the percolation temperature is $k_B T_p/J = 2.73 \pm 0.03$ coincident with the estimates of T_s . Therefore the percolation transition coincides with the 2-states Potts transition.

B. The first-order transition for $s = 7, 20$ and 50

For the $s = 7, 20$ and 50 cases we have considered systems with L from 10 to 50 lattice steps with p.b.c. On the base of the MF results [33] for the PFF model and the knowledge of the Potts model [26], we expect that the order of transition changes for $s > 4$. In fact, as it is shown in Figs. 10, M and E become more and more discontinuous as s increases. At the same time the percolation quantities develop better and better pronounced discontinuities (see Figs. 11).

In particular, the study of the Binder's parameter V reveals that the PFF model for $s = 7, 20$ and 50 has a first-order phase transition, since, for each considered lattice size L between 10 and 50, V has a non vanishing minimum, as shown in Fig. 12 - 14. In this cases the estimates of infinite size transition temperatures $T_s(s)$ and $T_p(s)$, for the thermodynamic and the percolation transition respectively, can be done through the relation [40]

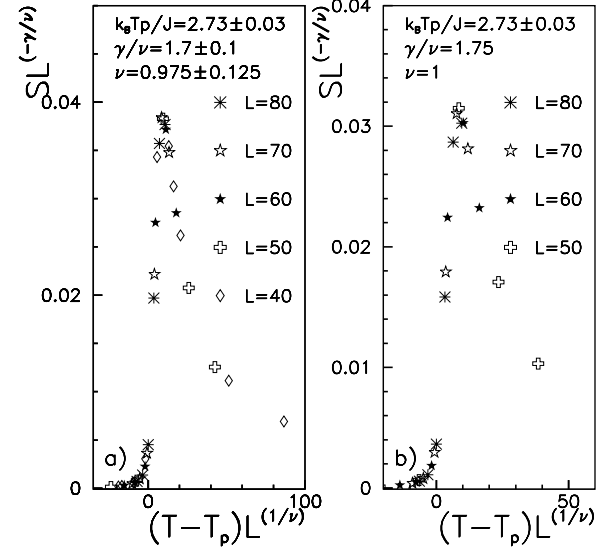


FIG. 9. PFF model with $s = 2$. Collapse of S data in Fig. 7: in panel a) for $L \geq 40$ with estimates of scaling parameters given in the figure; in b) for $L \geq 50$ for the Ising critical exponents and $k_B T_s/J = 2.73 \pm 0.03$ [41].

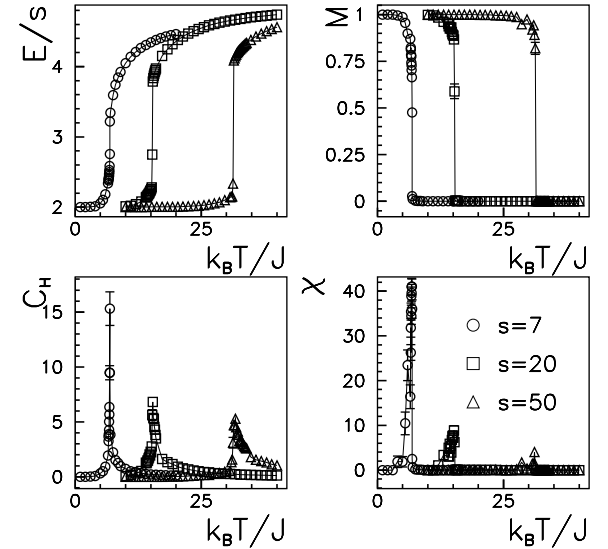


FIG. 10. PFF model with $s = 7, 20, 50$ and $L = 50$: Thermodynamic quantities as in Fig. 2. Lines are only guides for the eyes.

$$T_{\max}(L) - T_{\max}(\infty) \sim L^{-D} \quad (19)$$

where D is the Euclidean dimension, $T_{\max}(L)$ is the finite size temperature of the maximum of C_H and S respectively, and $T_{\max}(\infty)$ is the corresponding value in the thermodynamic limit. Therefore $T_s(s)$ and $T_p(s)$ can be evaluated by linear fits with one free parameter. The results are summarized in Tab. I.

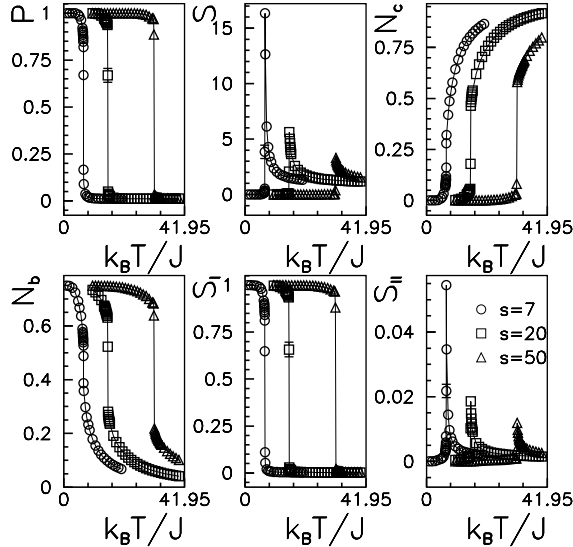


FIG. 11. PFF model with $s = 7, 20, 50$ and $L = 50$: Percolation quantities as in Fig. 7. Lines are only guides for eyes.

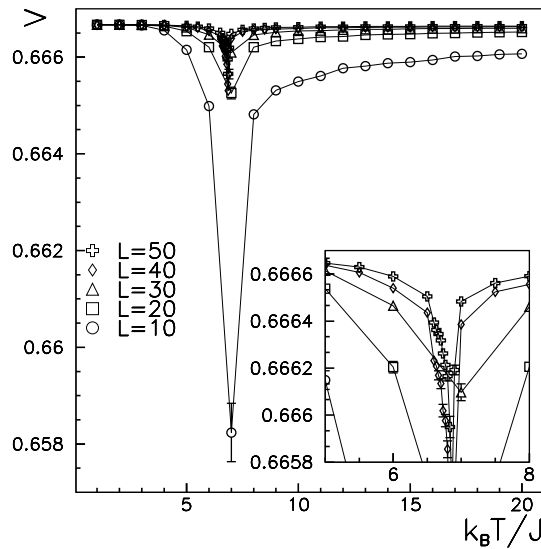


FIG. 12. PFF model with $s = 7$: Binder's parameter V as in Fig. 3.

C. Phase diagram

The numerical results in Secs. III A and III B give rise to a phase diagram for the PFF model (Fig. 15) qualitatively similar to the phase diagram of the PSG model. There is a high temperature phase, where both Ising spins and Potts variables are disordered, separated from a lower temperature phase by a Potts transition

where the Potts variables are ordered but the Ising spins (frustrated) are not, down to a second-order phase transition at T_{FF} where the correlation length of the Ising spins diverges. Notice that in more than 2D T_{FF} occurs at a s -dependent non-zero temperature. For example for $s = 1$ (FF Ising model) on a cubic lattice there is a second order phase transition at $k_B T / J \simeq 1.35$ [44]. Furthermore, the Potts transition numerically coincides with the percolation transition of the FK-CK clusters and, when the transition is of second-order (that is for $s \leq 4$ in 2D [26]), the set of Potts critical exponents coincides with the set of percolation exponents, confirming the MF calculation [33]. This result means that the FK-CK clusters represent the regions of correlated Potts variables, i.e. the cluster's characteristic linear size is equal to the correlation length of the Potts variables. As for the PSG model [12], also in this case a fit of $T_s(s) \equiv T_p(s)$ with the form

$$\frac{k_B T_p}{2saJ} = \frac{1}{\ln(1 + \sqrt{2sa})}, \quad (20)$$

with $a = 0.697 \pm 0.003$, works very well (see Fig. 15). The Eq. (20) is obtained from the exact expression of the transition temperature of the ferromagnetic $2s$ -state Potts model [26] only by renormalizing the number of states with a constant. Notice that in the PSG case the constant is equal to a greater value (0.800 ± 0.003) [12]. Hereafter we use the symbol T_p to identify both the Potts and the percolation transition.

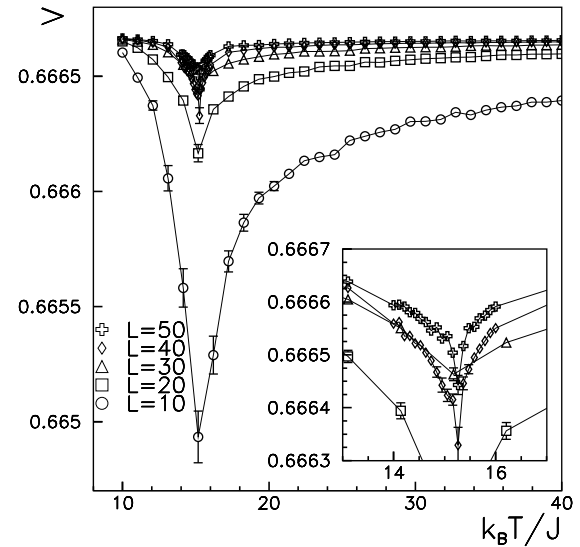


FIG. 13. PFF model with $s = 20$: Binder's parameter V as in Fig. 3.

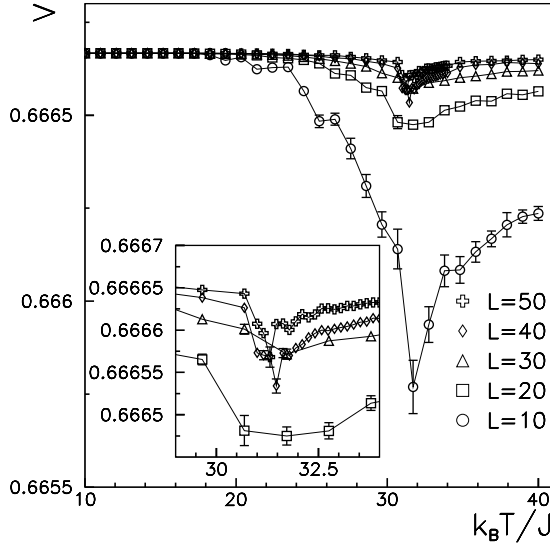


FIG. 14. PFF model with $s = 50$: Binder's parameter V as in Fig. 3.

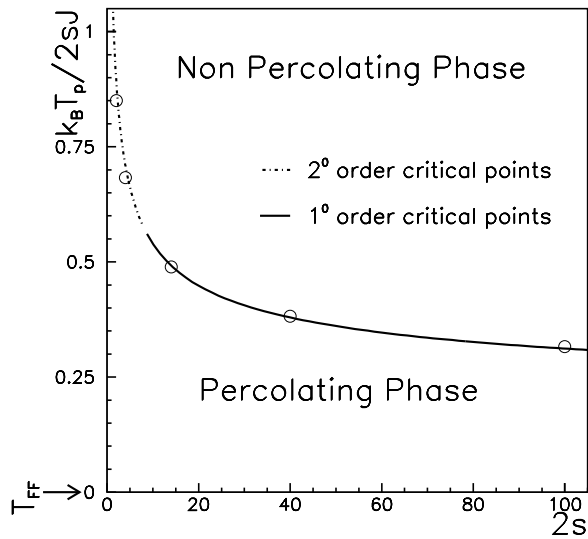


FIG. 15. PFF model: Numerical phase diagram in 2D. The data are fitted with Eq. (20) with $a = 0.697 \pm 0.003$. Data for $s = 1$ is from Ref. [37]. The errors are smaller than symbols size.

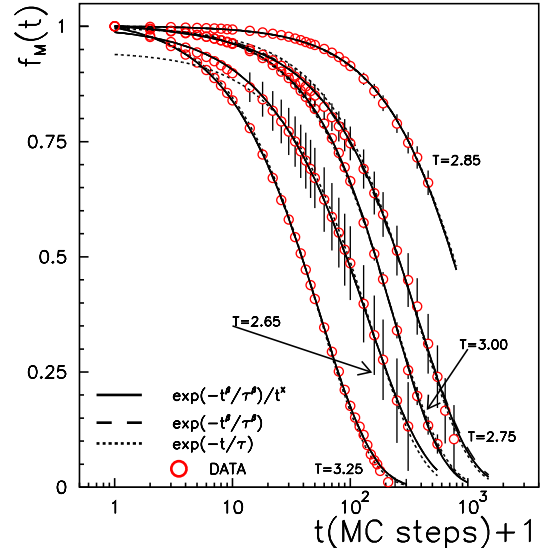


FIG. 16. PFF model with $s = 2$: Autocorrelation function of the Potts order parameter M in the thermodynamic limit (see text). For clarity we show only some of the recorded data for the simulated temperatures. Symbols are results of simulations, solid lines are fits with the form in Eq. (21), dash lines (on this scale indistinguishable from solid lines) with stretched exponential form and dotted lines with exponential form. Where not shown, the errors are smaller than the symbols size.

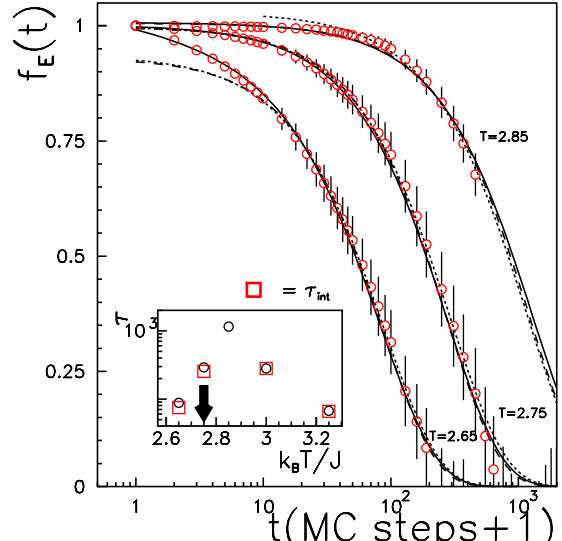


FIG. 17. PFF model with $s = 2$: Autocorrelation function of the energy density E in the thermodynamic limit (see text). For clarity we show only some of the recorded data for some of the simulated temperatures. Symbols are like in the Fig. 18. Inset: the autocorrelation times estimated by exponential fit (open circles) and by Eq. (23) (open squares). The arrow shows the numerical estimate of T_p . Where not shown, errors are smaller than symbols sizes.

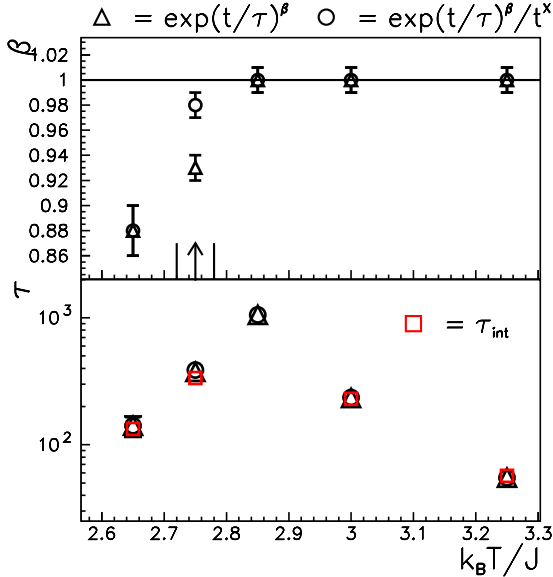


FIG. 18. PFF model with $s = 2$: Fit parameters for f_M data with form in Eq. (21) (open circles) and for stretched exponential form (open triangles). In the lower panel we show also the integral autocorrelation times τ_{int} estimated with the Eq. (23) (open squares). The arrow and the vertical lines show T_p and the numerical indetermination on it. Where not shown, errors are smaller than symbols sizes.

IV. DYNAMICAL BEHAVIOR FOR THE $S = 2$ CASE

In the $s = 2$ case the PFF model has a second-order Potts transition at $k_B T_p/J = 2.73 \pm 0.03$, as we have shown in Sec. III A. Therefore the correlation length of the Potts variables diverges and we expect a slowing down in the dynamics of these variables. Furthermore, in Ref. [13] we have seen that the Ising spins undergo to a dynamical transition at a temperature $T^* \simeq T_p$ characterized by a transition of the autocorrelation function of the non-linear susceptibility from a simple exponential function above T^* to a non-exponential function below T^* . In particular, the form suggested by Ogielski [25]

$$f(t) = f_0 \cdot \frac{e^{-(t/\tau)^\beta}}{t^x}, \quad (21)$$

that is a combination of a Kolraush-Williams-Watts stretched exponential function with a power law (where t is the time and f_0 , τ , x and β are constant), turns out to describe very well the autocorrelation function considered [13].

To test the critical dynamics and the form of autocorrelation functions related to the Potts variables we have simulated the PFF model (with $L = 20, 24, 30, 40$ and 50 lattice steps) with a standard local spin-flip dynamics [40] with an annealing method and 10^4 equilibration MC steps (defined as the update of the whole

system) at each temperature and averaging the data over more than 10^6 MC steps, for the temperature range $2.65 < k_B T/J < 3.25$ including T_p . We have calculated the autocorrelation function for the Potts order parameter M (that is a measure related to the Potts variables) and for the energy density E (that depends on both Ising spins and Potts variables). The autocorrelation function for a generic observable A is defined as

$$f_A(t) = \frac{\langle \delta A(t) \delta A(0) \rangle}{\langle (\delta A)^2 \rangle}, \quad (22)$$

where $\delta A(t) = A(t) - \langle A \rangle$. To extrapolate the data in the infinite size limit we have plotted at every time t the generic $f_A(t, L)$ for finite size L versus $1/L$, following the procedure suggested in Ref. [45]. The results are shown in Figs. 16 and 17.

To check the form of f_M and f_E we have fitted the data with three different plausible functions: *a*) simple exponential $f_0 \cdot \exp(-t/\tau)$; *b*) stretched exponential $f_0 \cdot \exp[-(t/\tau)^\beta]$ and *c*) Ogielski form in Eq. (21). Notice that for the form *c*) it is possible to estimate f_0 and x separately from β and τ , since the first two describe the short time behavior while the second two the long time regime. The resulting fits are drawn in Figs. 16 and 17.

Both f_M and f_E have an autocorrelation time that increases as the temperature approaches the critical region near T_p . In Figs. 17 and 18 it is shown also the integral autocorrelation time defined as

$$\tau_{int} = \lim_{t_{max} \rightarrow \infty} \frac{1}{2} + \sum_{t=0}^{t_{max}} f(t) \quad (23)$$

where f is the generic correlation function. The results are consistent with the estimated fits parameters τ . Therefore both the quantities M and E related to the Potts variables show a critical behavior as expected, while the autocorrelation of non-linear susceptibility has no such critical behavior at T_p [13], depending only on Ising spins which are not critical at T_p [13]. The forms *b*) and *c*) give always compatible estimates of β exponent, consistently with the very low values of x (that is approximately the slope of the function at $t = 0$). Below the Potts transition it is possible to see that the parameter β estimated using forms *b*) and *c*) for f_M becomes less than one, showing a dynamical transition between a high temperature single exponential autocorrelation to a low temperature stretched exponential autocorrelation function. This result confirms the presence of a complex dynamics below T_p evidenced also by the analysis of non-linear susceptibility correlation function [13]. On the other hand the data for f_E show that the long-time behavior is well described by an exponential function within the range of simulated temperatures and that the form *b*) with $\beta = 1$ and a non-zero x fits also the data for the lowest temperature.

V. SUMMARY AND CONCLUSIONS

One of the common features of the glassy systems is the occurrence at a temperature T^* , well above the glass transition, of precursor phenomena like the onset of long-time-regime non-exponential autocorrelation functions [2,28], well described by combination of a Kolraush-Williams-Watts stretched exponential function and a power law function as in Eq. (21). In spin systems with frustration this dynamical transition is well seen experimentally [22] and numerically [13,18,25]. The introduction [11] of a a generalization of $\pm J$ Ising spin glass (SG) and of fully frustrated (FF) Ising model, respectively the s -state Potts spin glass (PSG) [12] and Potts fully frustrated (PFF) model, allows to give an insight on the nature of this transition and on the relation between T^* and the phase transitions of these models [13,18].

In the present paper we have extensively studied in 2D, by means of efficient cluster Monte Carlo dynamics, the s -state PFF model, that recovers the FF Ising model for $s = 1$, showing that at a temperature $T_p(s)$ above the standard FF transition there is a transition in the universality class of the s -state ferromagnetic Potts transition. This result is consistent with the mean field prediction [33]. Moreover, we have shown that this transition coincides with the percolation transition of the Fortuin-Kasteleyn-Coniglio-Klein clusters [35]. These clusters, while in unfrustrated systems describe the regions of correlated spins [35], in frustrated systems have a characteristic linear length greater than the Ising spin correlation length and for $s > 1$ correspond to the regions of correlated Potts spins on the sub-lattice of interactions satisfied by Ising spins [11]. The out-coming phase diagram is shown in Fig. 15 and is qualitatively analogous to the phase diagram of the PSG model [12].

On the other hand the PFF and the PSG have different dynamical behaviors (simulated by means of spin-flip dynamics). All the results on the PSG model for $s = 2$ [13] and $s = 1$ (Ising SG) [25] show that a dynamical transition occurs in correspondence of the Griffiths temperature $T_c(s) > T_p(s)$, that is the ordering temperature of the unfrustrated regions allowed by the quenched disorder [23,24]. The Griffiths transition is a vanishing transition (for vanishing external magnetic field) at any s , therefore at $T_c(s)$ there is only an *essential* free energy singularity and the dynamical transition is consequence of the corrugation of free energy landscape [23].

In PFF model, where instead T_c is not defined for the absence of disorder, present results for $s = 2$ show that the autocorrelation function of the Potts order parameter M undergoes to a dynamical transition near T_p as well as the autocorrelation function of non-linear susceptibility (which has an explicit dependence only on the Ising spin) [13]. In this case at $T_p(s)$ a *real* thermodynamic transition occurs with a free energy singularity

at any integer $s > 1$, and for $s \leq 4$ there are diverging correlation times (and free energy barriers), as the computation of quantities depending on the Potts variables (e.g. M and E) reveals. Nevertheless also the dynamics of non-critical Ising spins is affected by the slowing down of critical Potts variables dynamics, as the onset of stretched exponentials on non-linear susceptibility shows [13]. What is interesting to note is that the dynamical transition at $T_p(s)$ persists also for $s = 1$ [18]. In this case T_p corresponds only to a percolation transition (defined for any s and coincident to the Potts transition for integer $s > 1$) and there is no free energy singularity at T_p , but the presence of a complex dynamics reveals that near T_p there is a change in the free energy landscape.

In conclusion the s -states PSG and PFF systems can be considered schematic models for glasses where frustrated orientational degrees of freedom, associated to s -states Potts variables, induce complex dynamics. The frustration is taking into account by means of frustrated Ising spins, with or without disordered interactions, and can be associated for example to steric hindrance. The study of these models shows that the fluctuations (χ and C_H) of orientational degrees of freedom diverge at $T_p(s)$ (for $s \leq 4$) as well as the related autocorrelation times (for f_M and f_E), while fluctuations and autocorrelation times of non-linear susceptibility depending directly only on the Ising spins [13] diverge at a lower glass transition temperature (the SG or FF transition temperature in these models) [46]. The diverging fluctuations at upper and lower transition temperatures are expected to be experimentally observable only using specific probes that couple with them. Examples of such probes could be those associated to dielectric measurements in supercooled-liquids and plastic glassy crystals [29–31] or to electron spin resonance spectroscopy measurements [28]. Moreover the model shows that, while in the presence of frustration and disorder the onset of complex dynamics is associated to the Griffiths transition (vanishing for any s), in frustrated systems with orientational degrees of freedom ($s > 1$) and without disorder this onset is related to a real thermodynamic Potts transition and for $s = 1$ to a vanishing Potts transition corresponding to a percolation transition. Finally, it is interesting to note that dielectric spectroscopy measurements in microemulsions and porous glasses [32] reveal that non-exponential autocorrelation functions occur at a percolation temperature like in the PFF model presented here.

ACKNOWLEDGMENTS

We are grateful to A. Coniglio for many stimulating observations. We would like also to thank Y. Feldman for interesting discussion and A. Scala for a critical reading of the manuscript. Partial support was given by the

[1] See for example *Proceedings of 14th Citges Conferences on Complex Behavior of Glassy Systems*, (Springer-Verlag, Berlin, 1996).

[2] C.A. Angell in *Relaxation in Complex Systems*, ed. by K.L. Ngai and G.B. Wright (Office of Naval Research, Washington, 1984); C.A. Angell, *Science* **267**, 1924 (1995); M.D. Ediger, C.A. Angell, and S.R. Nagel, *J. Phys. Chem* **100**, 13 200 (1996); C.A. Angell, *J. Non-Cryst. Sol.* **102**, 205 (1988).

[3] W.Götze, in *Liquids, freezing and glass transition*, Les Housches, ed. by J.P. Hansen, D. Levesque, J. Zinn-Justin (North Holland, Amsterdam, 1989).

[4] See for example L.C.E. Struik, *Physical Aging in Amorphous Polymers and Other Materials*, (Elsevier, Amsterdam, 1978).

[5] K. Binder e A.P. Young, *Rev. Mod. Phys.* **58**, 801 (1986) and references therein; M. Mezard, G. Parisi, and M.A. Virasoro, *Spin Glass Theory and Beyond* (World Scientific, Singapore, 1987); K.H. Fischer and J.A. Hertz, *Spin Glasses* (Cambridge University Press, Cambridge, 1991); *Spin Glasses and Random Fields*, ed. by A.P. Young (World Scientific, Singapore, 1998).

[6] R. Rammal and J.Souletie, in *Magnetism of Metals and Alloys*, ed. M. Cyrot (North-Holland, Amsterdam, 1982).

[7] See for example D.L Stein and R.G. Palmer, *Phys. Rev. B* **38**, 12035 (1988) and reference therein; G. Parisi, *Phys. Rev. Lett.* **79**, 3660 (1997).

[8] H. Tanaka, *J. Phys. Condens. Matter* **10**, L207 (1998).

[9] See for example T.R. Kirkpatrick and D. Thirumalai, *J. Phys. A* **22**, L149 (1989) and *Transp. Theor. Stat. Phys.* **24**, 927 (1995); L.F. Cugliandolo, J. Kurchan, G. Parisi, and F. Ritort, *Phys. Rev. Lett.* **74**, 1012 (1995); S. Franz and G. Parisi, *Phys. Rev. Lett.* **79**, 2486 (1997).

[10] J.P. Bouchaud, L. Cugliandolo, J. Kurchan, M. Mezard in *Spin Glasses and Random Fields*, ed. by A.P. Young (World Scientific, Singapore, 1998).

[11] A. Coniglio, F. di Liberto, G. Monroy, and F. Peruggi, *Phys. Rev. B* **44**, 12 605 (1991).

[12] G. Franzese and A. Coniglio, *Phys. Rev. E* **58**, 2753 (1998).

[13] G. Franzese and A. Coniglio, in print on *Phys. Rev. E*.

[14] There is a complementary way to introduce the frustration in glass models, considering trivial Hamiltonian with kinetics constrains as geometrical hindrance (see for example Ref. [15]). The relation between geometrical frustration and energetic frustration is one of the open questions.

[15] J. Jäckle, *Prog. Theor. Phys. Supplement* **126**, 53 (1997) and reference therein.

[16] J.P. Bouchaud and M. Mezard, *J. Phys. I* **4**, 1109 (1994); S. Franz and J. Hertz, *Phys. Rev. Lett.* **74**, 2114 (1995); E. Marinari, G. Parisi, and F. Ritort, *J. Phys. A* **28**, 327 (1995); P. Chandra, L.B. Ioffe, D. Sherrington, *Phys. Rev. Lett.* **75**, 713 (1995); P. Chandra, M.V. Feigelman, L.B. Ioffe, *Phys. Rev. Lett.* **76**, 4805 (1996); D.M. Kagan, L.B. Ioffe, M.V. Feigelman, Preprint cond-mat/9902175.

[17] J. Villain, *J. Phys. C* **10**, 1717 (1977).

[18] A. Fierro, G. Franzese, A. de Candia, and A. Coniglio, *Phys. Rev E* **59**, 60 (1999).

[19] B. Kim and S.J. Lee, *Phys. Rev. Lett.* **79**, 3709 (1997); S.J. Lee and B. Kim, Preprint cond-mat/9901077.

[20] See for example Proceedings of the ICTP Workshop on *Josephson Junction Arrays*, ed. by H.A. Cerdeira and S.R. Shenoy, *Physica B* **222**, 253 (1996).

[21] This dynamical anomaly is present also in the Ising model, but only in two dimensions as theoretical and numerical works have shown. See D. Stauffer, *Physica A* **186**, 197 (1992) and P. Grassberger and D. Stauffer, *Physica A* **232**, 171 (1996).

[22] See for example P. Granberg, P. Svendlindh, P. Norblad, and L. Lundgren, in *Heidelberg Colloquium on Glassy Dynamics*, ed. by J.L. van Hemmen and I. Morgenstern (Springer-Verlag, Berlin, 1987), P. Refrigier, E. Vincent, M. Ocio, and J. Hamman, *Jpn. J. Appl. Phys.* **26**, Suppl. 3, 783 (1987).

[23] M. Randeria, J.P. Sethna, and R.G. Palmer, *Phys. Rev. Lett.* **57**, 245 (1986); A. Bray, *Phys. Rev. Lett.* **59**, 586 (1987); F. Cesi, C. Maes, and F. Martinelli, *Commun. Math. Phys.* **188**, 135 (1997).

[24] R.B. Griffiths, *Phys. Rev. Lett.* **23**, 17 (1969).

[25] A.T. Ogielski, *Phys. Rev. B* **32**, 7384 (1985).

[26] F. Wu, *Rev. Mod. Phys.* **54**, 235 (1982).

[27] The clusters defined by this percolation are at the base of the efficiency of the used cluster MC dynamics, as shown in Ref. [12].

[28] L. Andreozzi, N. Giordano, D. Leporini, *J. Non-Cryst. Sol.* **235**, 219 (1998).

[29] P.K. Dixon, L. Wu, S.R. Nagel, B.D. Williams, and J.P. Carini, *Phys. Rev. Lett.* **65**, 1108 (1990) and **66**, 960 (1991).

[30] E.W. Fisher, E. Donth, and W. Steffen, *Phys. Rev. Lett.* **68**, 2344 (1992); N. Menon and S.R. Nagel, *Phys. Rev. Lett.* **74**, 1230 (1995).

[31] H. Suga, in *Slow Dynamics in Condensed Matter*, Proceedings of The First Tohwa International Symposium (American Institute of Physics, New York, 1991); D.L. Leslie-Pelecky and N.O. Birge, *Phys. Rev. Lett.* **72**, 1232 (1994) and *Phys. Rev. B* **50**, 13250 (1994); R. Brand, P. Lunkenheimer, and A. Loidl, *Phys. Rev. B* **56**, R5713 (1997).

[32] Y. Feldman, N. Kozlovich, and Y. Alexandrov, *Phys. Rev. E* **54**, 5420, (1996); A. Puzenko, N. Kozlovich, A. Gutina, and Y. Feldman, *Determination of pore fractal dimensions and porosity of silica glasses from the dielectric response at percolation*, preprint.

[33] F. di Liberto and F. Peruggi, *Physica A* **248**, 273 (1998).

[34] A renormalization group analysis is done in U. Pezzella and A. Coniglio, *Physica A* **237**, 353 (1997); a replica approach gives same qualitative results (M. Sellitto, private communication, 1996).

[35] C.M. Fortuin and P.W. Kasteleyn, *Physica* **57**, 536 (1972); A. Coniglio and W. Klein, *J.Phys.A* **13**, 2775 (1980).

[36] G. Andre et al. *Jour. Phys. (Paris)*, **40**, 479 (1979);

G. Forgacs, Phys. Rev. B **22**, 4473 (1980).

[37] V. Cataudella, Physica A, **183**, 249 (1992).

[38] R.H. Swendsen and J.S. Wang, Phys. Rev. Lett. **58**, 86 (1987).

[39] K. Binder, Z. Phys. B **43**, 119 (1981).

[40] K. Binder and D.W. Hermann, *Monte Carlo Simulation in Statistical Physics*, (Springer-Verlag, Berlin, 1988).

[41] The errors on scaling parameters are estimated as ranges within which, varying a parameter and taking all the others fixed, one can obtain a good data collapse.

[42] E. Stanley, *Introduction to Phase Transitions and Critical Phenomena* (Calendron Press, Oxford, 1971).

[43] A. Aharony, and D. Stauffer, *Introduction to Percolation Theory* (Taylor & Francis, 1994).

[44] H. Diep, P. Lallemand, and O. Nagai, J. Phys. C **18**, 1067 (1985); G.S. Grest, J. Phys. C **18**, 6239 (1985); L.W. Bernardi, K. Hukushima, H. Takayama J. Phys. A **32**, 1787 (1999).

[45] I.A. Campbell and L. Bernardi, Phys. Rev. B **50**, 12 643 (1994).

[46] We expect that a quantity depending on both types of spins, like the energy E , shows diverging autocorrelation times also at the lower transition temperature.

TABLE I. PFF model: Numerical estimates of thermodynamic transition temperature T_s and percolation transition temperature T_p for $s = 7, 20, 50$.

s	T_s	T_p
7	6.87 ± 0.04	6.85 ± 0.06
20	15.3 ± 0.1	15.3 ± 0.1
50	31.7 ± 0.1	31.5 ± 0.1